

Extended Block-Lifting-Based Lapped Transforms

著者別名	鈴木 大三, 工藤 博幸
journal or publication title	IEEE signal processing letters
volume	22
number	10
page range	1657-1660
year	2015-10
権利	(C) 2015, IEEE. Personal use of this material is permitted. Permission from IEEE must be obtained for all other uses, in any current or future media, including reprinting /republishing this material for advertising or promotional purposes, creating new collective works, for resale or redistribution to servers or lists, or reuse of any copyrighted component of this work in other works.
URL	http://hdl.handle.net/2241/00124676

doi: 10.1109/LSP.2015.2422837

Extended Block-Lifting-based Lapped Transforms

Taizo Suzuki, *Member, IEEE* and Hiroyuki Kudo, *Member, IEEE*

Abstract—We extend an original lapped transform (LT) and use block-lifting factorization to get an extended block-lifting-based LT (XBL-LT). The block-lifting structure maps integer input signals to integer output signals and results in a reversible transform that reduces rounding errors by merging many rounding operations. Although other such block-lifting-based LTs (BL-LTs) have been proposed, they are forcibly constrained by the use of discrete cosine transform (DCT) matrices. In contrast, XBL-LT is DCT-unconstrained and hence also embodies the DCT-constrained form. Furthermore, it has fewer rounding operations by merging the scaling factor with block-lifting coefficients. The both DCT-constrained and unconstrained XBL-LTs perform well at lossy-to-lossless image coding which has scalability from lossless data to lossy data.

Index Terms—Block-lifting structure, lapped transform (LT), lossy-to-lossless image coding

I. INTRODUCTION

LAPPED transforms (LTs) [1] are popular subband transforms that can be used as substitutes for the discrete cosine transform (DCT) [2] used in image/video compression (image coding). Although almost all of the JPEG and H.26x series [3–5], image coding standards, use DCTs for their good energy compaction, DCT-based image codings generate unpleasant artifacts, i.e., blocking artifacts, at low bit rates due to their ignoring the continuity of the blocks. LT-based image coding solves that problem by using a processing that works over the blocks.

The lifting structure [6] is a very important technology to achieve a lossless mode in subband transform-based image coding. It maps integer input signals to integer output signals; i.e., it is an integer-to-integer transform. The 4×8 lifting-based LT (L-LT) [7] in JPEG XR [8], the newest image coding standard, is a time-domain LT (TDLT) [9] with simple scaling factors and lifting structures. In spite of its simple structure, it performs well at lossy-to-lossless image coding, which has scalability from lossless to lossy data. The block-lifting structure [10] is a class of lifting structures and results in a reversible transform that reduces rounding errors by merging many rounding operations. Inspired by the L-LT in JPEG XR, we have proposed block-lifting-based LTs (BL-LTs) [11], [12] that perform well with larger block size than those of the L-LT in JPEG XR. However, they are forcibly DCT-constrained and degrade coding performance at high bit rates.

Here, we extend an original LT and use block-lifting factorization to get an extended BL-LT (XBL-LT). The XBL-LT is DCT-unconstrained, unlike the BL-LTs presented in [11], [12], and hence also embodies the DCT-constrained form. Furthermore, more rounding operations than the methods

described in our previous studies are removed by merging the scaling factor with block-lifting coefficients. As a result, the both DCT-constrained and unconstrained XBL-LTs perform well at lossy-to-lossless image coding.

Notation: The italic letter M ($M = 2^n$, $n \in \mathbb{N}$) denotes the block size. Boldface letters \mathbf{I}_m , \mathbf{J}_m , $\mathbf{0}$, and \mathbf{D}_m denote an $m \times m$ identity matrix, an $m \times m$ reversal matrix, a null matrix, and an $m \times m$ diagonal matrix with alternating ± 1 entries (i.e., $\text{diag}\{1, -1, 1, -1, \dots\}$), respectively. The superscripts T and -1 respectively mean the transpose and inverse of a matrix.

II. REVIEW AND DEFINITION

A. Lapped Transform (LT)

In accordance with [11], [12], let $\mathbf{E}(z)$ be a polyphase matrix of an $M \times 2M$ LT with a scaling factor s derived from the L-LT in JPEG XR [7]:

$$\mathbf{E}(z) = \mathbf{P} \begin{bmatrix} \mathbf{I}_N & \mathbf{0} \\ \mathbf{0} & \mathbf{S}_N^{\text{IV}} \mathbf{C}_N^{\text{III}} \end{bmatrix} \Gamma(z) \begin{bmatrix} \mathbf{C}_N^{\text{II}} & \mathbf{0} \\ \mathbf{0} & \mathbf{C}_N^{\text{IV}} \mathbf{J}_N \end{bmatrix} \widetilde{\mathbf{S}} \mathbf{W} \mathbf{J}_M, \quad (1)$$

where

$$\begin{aligned} \Gamma(z) &= \mathbf{W} \Lambda(z) \mathbf{W}, \quad \Lambda(z) = \text{diag}\{\mathbf{I}_N, z^{-1} \mathbf{I}_N\} \\ \mathbf{W} &= \frac{1}{\sqrt{2}} \begin{bmatrix} \mathbf{I}_N & \mathbf{I}_N \\ \mathbf{I}_N & -\mathbf{I}_N \end{bmatrix}, \quad \widetilde{\mathbf{W}} = \frac{1}{\sqrt{2}} \begin{bmatrix} \mathbf{I}_N & \mathbf{J}_N \\ \mathbf{J}_N & -\mathbf{I}_N \end{bmatrix} \\ \mathbf{S} &= \text{diag}\{s \mathbf{I}_N, s^{-1} \mathbf{I}_N\}. \end{aligned}$$

\mathbf{C}_M^X and \mathbf{S}_M^X are type- X DCT (DCT- X) and type- X discrete sine transform (DST- X) matrices, and the (i, j) -elements of \mathbf{C}_M^{II} and \mathbf{C}_M^{IV} are

$$\begin{aligned} [\mathbf{C}_M^{\text{II}}]_{i,j} &= \sqrt{\frac{2}{M}} c_i \cos\left(\frac{i(j+1/2)\pi}{M}\right) \\ [\mathbf{C}_M^{\text{IV}}]_{i,j} &= \sqrt{\frac{2}{M}} \cos\left(\frac{(i+1/2)(j+1/2)\pi}{M}\right), \end{aligned}$$

where $c_k = 1/\sqrt{2}$ ($k = 0$) or 1 ($k \neq 0$), respectively. The following relationships between matrices can be established:

$$\mathbf{C}_M^{\text{III}} = \left(\mathbf{C}_M^{\text{II}}\right)^{-1} = \left(\mathbf{C}_M^{\text{II}}\right)^T, \quad \mathbf{S}_M^{\text{IV}} = \mathbf{D}_M \mathbf{C}_M^{\text{IV}} \mathbf{J}_M. \quad (2)$$

Here, \mathbf{P} is an $M \times M$ permutation matrix. The optimal scaling s in \mathbf{S} is empirically determined, e.g., $s = 0.8981$ if $M = 8$ and 0.9360 if $M = 16$. Since the LT in Eq. (1) with $s = 1$ is completely equivalent to a lapped orthogonal transform (LOT), we will use the LT in Eq. (1) as a representative expression of LT.

T. Suzuki and H. Kudo are with the Faculty of Engineering, Information and Systems, University of Tsukuba, Tsukuba, Ibaraki, 305-8573 Japan (e-mail: {taizo, kudo}@cs.tsukuba.ac.jp).

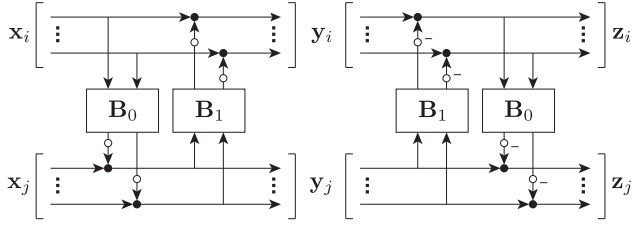


Fig. 1. Block-lifting structure (black and white circles mean adders and rounding operations, respectively).

B. Block-Lifting Structure

The block-lifting structure [10] (Fig. 1) is a class of lifting structures. The structure can be expressed as follows:

$$\begin{aligned} \mathbf{y}_j &= \mathbf{x}_j + \text{round}(\mathbf{B}_0 \mathbf{x}_i), & \mathbf{y}_i &= \mathbf{x}_i + \text{round}(\mathbf{B}_1 \mathbf{y}_j) \\ \mathbf{z}_i &= \mathbf{y}_i - \text{round}(\mathbf{B}_1 \mathbf{y}_j) = \mathbf{x}_i, & \mathbf{z}_j &= \mathbf{y}_j - \text{round}(\mathbf{B}_0 \mathbf{z}_i) = \mathbf{x}_j, \end{aligned}$$

where \mathbf{x}_\times , \mathbf{y}_\times , and \mathbf{z}_\times are $N \times 1$ input/output vector signals, $\text{round}(\cdot)$ is a rounding operation, and the block-lifting coefficients \mathbf{B}_0 and \mathbf{B}_1 are $N \times N$ arbitrary matrices. In this case, the matrices and their inverses are expressed as lower and upper block-lifting matrices as follows:

$$\begin{aligned} \mathfrak{L}[\mathbf{B}_0] &\triangleq \begin{bmatrix} \mathbf{I}_N & \mathbf{0} \\ \mathbf{B}_0 & \mathbf{I}_N \end{bmatrix}, & \mathfrak{L}[\mathbf{B}_0]^{-1} &= \mathfrak{L}[-\mathbf{B}_0] \\ \mathfrak{U}[\mathbf{B}_1] &\triangleq \begin{bmatrix} \mathbf{I}_N & \mathbf{B}_1 \\ \mathbf{0} & \mathbf{I}_N \end{bmatrix}, & \mathfrak{U}[\mathbf{B}_1]^{-1} &= \mathfrak{U}[-\mathbf{B}_1]. \end{aligned}$$

Rounding errors generated by the rounding operation in each lifting step degrade coding performance. The block-lifting structure reduces such rounding errors by merging many rounding operations. A special class of block-lifting structure is expressed as [13]

$$\begin{aligned} \begin{bmatrix} \mathbf{M} & \mathbf{0} \\ \mathbf{0} & \mathbf{M}^{-1} \end{bmatrix} &= \mathfrak{L}[\mathbf{M}^{-1}] \mathfrak{U}[-\mathbf{M}] \mathfrak{L}[\mathbf{M}^{-1}] \tilde{\mathbf{J}}_M & (3) \\ &= \hat{\mathbf{J}}_M \mathfrak{L}[-\mathbf{M}] \mathfrak{U}[\mathbf{M}^{-1}] \mathfrak{L}[-\mathbf{M}], & (4) \end{aligned}$$

where

$$\tilde{\mathbf{J}}_M = \begin{bmatrix} \mathbf{0} & \mathbf{I}_N \\ -\mathbf{I}_N & \mathbf{0} \end{bmatrix}, \quad \hat{\mathbf{J}}_M = \begin{bmatrix} \mathbf{0} & -\mathbf{I}_N \\ \mathbf{I}_N & \mathbf{0} \end{bmatrix},$$

and \mathbf{M} is an $N \times N$ arbitrary nonsingular matrix.

III. EXTENDED BLOCK-LIFTING-BASED LAPPED TRANSFORM (XBL-LT)

Theorem: We can extend the DCT-constrained LT in Eq. (1) to a DCT-unconstrained LT as follows:

$$\mathbf{E}(z) = \mathbf{P} \begin{bmatrix} \mathbf{I}_N & \mathbf{0} \\ \mathbf{0} & \mathbf{D}_N \tilde{\mathbf{V}}^{-1} \mathbf{J}_N \tilde{\mathbf{U}}^{-1} \end{bmatrix} \Gamma(z) \begin{bmatrix} \tilde{\mathbf{U}} & \mathbf{0} \\ \mathbf{0} & \tilde{\mathbf{V}} \mathbf{J}_N \end{bmatrix} \tilde{\mathbf{S}} \tilde{\mathbf{W}} \mathbf{J}_M,$$

where $\tilde{\mathbf{U}}$ and $\tilde{\mathbf{V}}$ are $N \times N$ arbitrary nonsingular matrices. This equation can be simplified as

$$\mathbf{E}(z) = \mathbf{P} \begin{bmatrix} \mathbf{I}_N & \mathbf{0} \\ \mathbf{0} & \mathbf{V}^{-1} \mathbf{J}_N \mathbf{U}^{-1} \end{bmatrix} \Gamma(z) \begin{bmatrix} \mathbf{U} & \mathbf{0} \\ \mathbf{0} & \mathbf{V} \mathbf{J}_N \end{bmatrix} \hat{\mathbf{W}} \mathbf{J}_M, \quad (5)$$

where

$$\mathbf{U} = \sqrt{2s} \tilde{\mathbf{U}}, \quad \mathbf{V} = \frac{1}{\sqrt{2s}} \tilde{\mathbf{V}}, \quad \hat{\mathbf{W}} = \begin{bmatrix} \frac{1}{2} \mathbf{I}_N & \frac{1}{2} \mathbf{J}_N \\ \mathbf{J}_N & -\mathbf{I}_N \end{bmatrix},$$

by using Eq. (2) and skipping the sign inversion matrix \mathbf{D}_N . The scaling matrix \mathbf{S} is being embedded in \mathbf{U} and \mathbf{V} . When $\tilde{\mathbf{U}} = \mathbf{C}_N^H$ and $\tilde{\mathbf{V}} = \mathbf{C}_N^V$, the LT in Eq. (5) is completely equivalent to the LT in Eq. (1) except that the signs are different. Then, we factorize the LT in Eq. (5) into block-lifting structures as

$$\begin{aligned} \mathbf{E}(z) &= \mathbf{P} \mathfrak{L}[\mathbf{B}_4] \mathfrak{U}[\mathbf{B}_3] \Lambda(z) \mathfrak{U}[\mathbf{B}_3] \mathfrak{L}[\mathbf{B}_2] \mathfrak{U}[\mathbf{B}_1] \mathfrak{L}[\mathbf{B}_0] \\ &\cdot \mathfrak{U} \left[-\frac{1}{2} \mathbf{J}_N \right] \mathfrak{L}[\mathbf{J}_N] \tilde{\mathbf{J}}_M, \end{aligned} \quad (6)$$

wherein each matrix is defined as

$$\begin{aligned} \mathbf{B}_0 &= -\mathbf{V}^{-1}, \quad \mathbf{B}_1 = \mathbf{V}, \quad \mathbf{B}_2 = \mathbf{B}_0 + \mathbf{B}_4 \\ \mathbf{B}_3 &= -\frac{1}{2} \mathbf{U} \mathbf{J}_N \mathbf{V}, \quad \mathbf{B}_4 = \mathbf{V}^{-1} \mathbf{J}_N \mathbf{U}^{-1}. \end{aligned}$$

Actually, the block-lifting matrices $\mathfrak{U}[\mathbf{B}_3]$ on both sides of the delay matrix $\Lambda(z)$ are collectively implemented, as shown in Fig. 2.

Proof: We can perform an easy matrix manipulation as follows:

$$\begin{aligned} \begin{bmatrix} \mathbf{M}_0 & \mathbf{0} \\ \mathbf{0} & \mathbf{M}_1 \end{bmatrix} \begin{bmatrix} \mathbf{I}_N & \mathbf{N}_0 \\ \mathbf{N}_1 & \mathbf{I}_N \end{bmatrix} \\ = \begin{bmatrix} \mathbf{I}_N & \mathbf{M}_0 \mathbf{N}_0 \mathbf{M}_1^{-1} \\ \mathbf{M}_1 \mathbf{N}_1 \mathbf{M}_0^{-1} & \mathbf{I}_N \end{bmatrix} \begin{bmatrix} \mathbf{M}_0 & \mathbf{0} \\ \mathbf{0} & \mathbf{M}_1 \end{bmatrix}, \end{aligned}$$

where \mathbf{M}_\times and \mathbf{N}_\times are an $N \times N$ arbitrary nonsingular matrix and $N \times N$ arbitrary matrix, respectively. First, $\Gamma(z)$ in Eq. (5) can easily be represented by

$$\Gamma(z) = \mathfrak{L}[\mathbf{I}_N] \mathfrak{U} \left[-\frac{1}{2} \mathbf{I}_N \right] \Lambda(z) \mathfrak{U} \left[\frac{1}{2} \mathbf{I}_N \right] \mathfrak{L}[-\mathbf{I}_N].$$

Next, \mathbf{U}^{-1} in Eq. (5) is moved to the right side of $\Gamma(z)$ and simplified as

$$\begin{aligned} \Psi(z) &\triangleq \begin{bmatrix} \mathbf{I}_N & \mathbf{0} \\ \mathbf{0} & \mathbf{U}^{-1} \end{bmatrix} \Gamma(z) \begin{bmatrix} \mathbf{U} & \mathbf{0} \\ \mathbf{0} & \mathbf{I}_N \end{bmatrix} \\ &= \mathfrak{L}[\mathbf{U}^{-1}] \mathfrak{U} \left[-\frac{1}{2} \mathbf{U} \right] \Lambda(z) \mathfrak{U} \left[\frac{1}{2} \mathbf{U} \right] \mathfrak{L}[-\mathbf{U}^{-1}] \begin{bmatrix} \mathbf{U} & \mathbf{0} \\ \mathbf{0} & \mathbf{U}^{-1} \end{bmatrix} \\ &= \mathfrak{L}[\mathbf{U}^{-1}] \mathfrak{U} \left[-\frac{1}{2} \mathbf{U} \right] \Lambda(z) \mathfrak{U} \left[-\frac{1}{2} \mathbf{U} \right] \mathfrak{L}[\mathbf{U}^{-1}] \tilde{\mathbf{J}}_M, \end{aligned}$$

because the block diagonal matrix $\text{diag}\{\mathbf{U}, \mathbf{U}^{-1}\}$ in $\Psi(z)$ can be factorized into block-lifting structures as in Eq. (3). Then, $\mathbf{V}^{-1} \mathbf{J}_N$ in Eq. (5) is moved to the right side of $\Psi(z)$ and

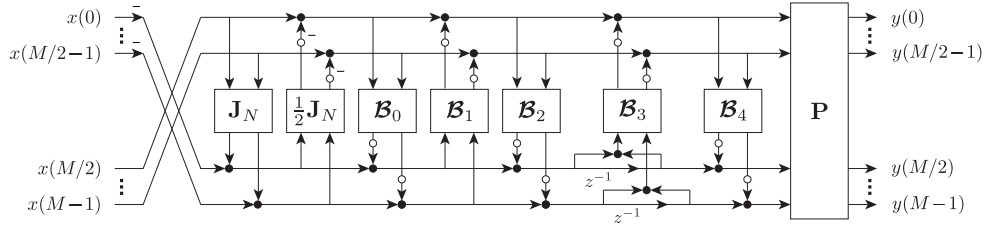


Fig. 2. XBL-LT (black and white circles mean adders and rounding operations, respectively).

TABLE I
CODING GAINS OF XBL-LTs.

Block Size	DCT-Constrained	DCT-Unconstrained
8	9.4475	9.4538
16	9.8455	9.8621

TABLE II
NUMBERS OF ROUNDING OPERATIONS OF BL-LTs.

Block Size	BL-LT [11]	BL-LT [12]	XBL-LT
8	48	28	24
16	96	56	48
M	$6M$	$7M/2$	$3M$

simplified as

$$\begin{aligned}
 \Omega(z) &\triangleq \begin{bmatrix} \mathbf{I}_N & \mathbf{0} \\ \mathbf{0} & \mathbf{v}^{-1} \mathbf{J}_N \end{bmatrix} \Psi(z) \begin{bmatrix} \mathbf{I}_N & \mathbf{0} \\ \mathbf{0} & \mathbf{v} \mathbf{J}_N \end{bmatrix} \\
 &= \mathfrak{L}[\mathbf{W}^{-1}] \mathfrak{U} \left[-\frac{1}{2} \mathbf{W} \right] \Lambda(z) \mathfrak{U} \left[-\frac{1}{2} \mathbf{W} \right] \\
 &\quad \cdot \mathfrak{L}[\mathbf{W}^{-1}] \tilde{\mathbf{J}}_M \begin{bmatrix} \mathbf{v}^{-1} \mathbf{J}_N & \mathbf{0} \\ \mathbf{0} & \mathbf{v} \mathbf{J}_N \end{bmatrix} \\
 &= \mathfrak{L}[\mathbf{W}^{-1}] \mathfrak{U} \left[-\frac{1}{2} \mathbf{W} \right] \Lambda(z) \mathfrak{U} \left[-\frac{1}{2} \mathbf{W} \right] \\
 &\quad \cdot \mathfrak{L}[\mathbf{W}^{-1} - \mathbf{v}^{-1}] \mathfrak{U}[\mathbf{v}] \mathfrak{L}[-\mathbf{v}^{-1}] \begin{bmatrix} \mathbf{J}_N & \mathbf{0} \\ \mathbf{0} & \mathbf{J}_N \end{bmatrix},
 \end{aligned}$$

where $\mathbf{W} = \mathbf{U} \mathbf{J}_N \mathbf{V}$, because the block diagonal matrix $\text{diag}\{\mathbf{v}^{-1}, \mathbf{v}\}$ in $\Omega(z)$ can also be factorized into block-lifting structures as in Eq. (4). Finally, the residual part $\widehat{\mathbf{W}} \mathbf{J}_M$ in Eq. (5) and $\text{diag}\{\mathbf{J}_N, \mathbf{J}_N\}$ in $\Omega(z)$ are collectively factorized as

$$\begin{bmatrix} \mathbf{J}_N & \mathbf{0} \\ \mathbf{0} & \mathbf{J}_N \end{bmatrix} \widehat{\mathbf{W}} \mathbf{J}_M = \mathfrak{U} \left[-\frac{1}{2} \mathbf{J}_N \right] \mathfrak{L}[\mathbf{J}_N] \tilde{\mathbf{J}}_M.$$

□

IV. EXPERIMENTAL RESULTS

A. Coding Gain, Frequency Response, and Number of Rounding Operations

We designed 8×16 and 16×32 XBL-LTs by optimizing the coding gain (CG) [14]

$$\text{CG [dB]} = 10 \log_{10} \frac{\sigma_x^2}{\prod_{k=0}^{M-1} \sigma_{x_k}^2 \|f_k\|^2},$$

where σ_x^2 is the variance of the input signal, $\sigma_{x_k}^2$ is the variance of the k -th subbands and $\|f_k\|^2$ is the norm of the k -th synthesis filter. To simplify the design in DCT-unconstrained

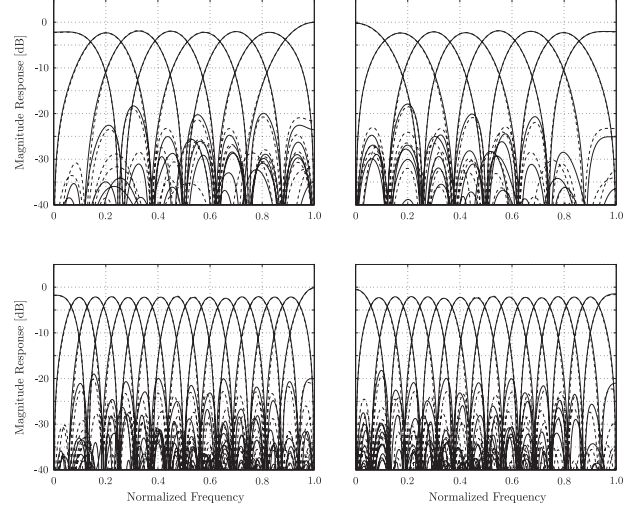


Fig. 3. Frequency responses of analysis and synthesis parts of XBL-LTs (dashed and solid lines indicate DCT-constrained and unconstrained cases, respectively): (top) 8×16 XBL-LT, (bottom) 16×32 XBL-LT.

case, we set $\tilde{\mathbf{U}}$ and $\tilde{\mathbf{V}}$ in Eq. (6) as $N \times N$ arbitrary unitary matrices, where $\tilde{\mathbf{U}}$ is designed such that it has structural one-degree regularity [10] to achieve good image coding. Table I compares of the CGs[dB] of the XBL-LTs in the DCT-constrained and unconstrained cases. In addition, Fig. 3 shows the frequency responses of the analysis and synthesis parts of the XBL-LTs for the same cases as in Table I. In Table I and Fig. 3, the DCT-unconstrained case had slightly better results than the DCT-constrained case. Table II shows the numbers of rounding operations of BL-LTs. It is clear that the XBL-LTs have fewer rounding operations than those of conventional BL-LTs.

B. Lossy-to-Lossless Image Coding

For convenience regarding the number of pages, lossy-to-lossless image coding was implemented in only the $M = 8$ case. We used L-LTs in [7], [9], [11], [12] as the conventional L-LTs. The L-LT in [7] is the 4×8 L-LT for JPEG XR. The L-LT in [9] is the 8×16 TDLT with the pre-filtering part indicated by Cfg. 5 in Table V in [9] and the DCT part indicated by [15]. The L-LTs in [11], [12] are the DCT-constrained BL-LTs. After the images were transformed by the L-LTs and periodic extension at the boundaries, the transformed coefficients were rearranged from the subband mode to the multiresolution mode similar to the wavelet transform. They were encoded with a common wavelet-based zerotree

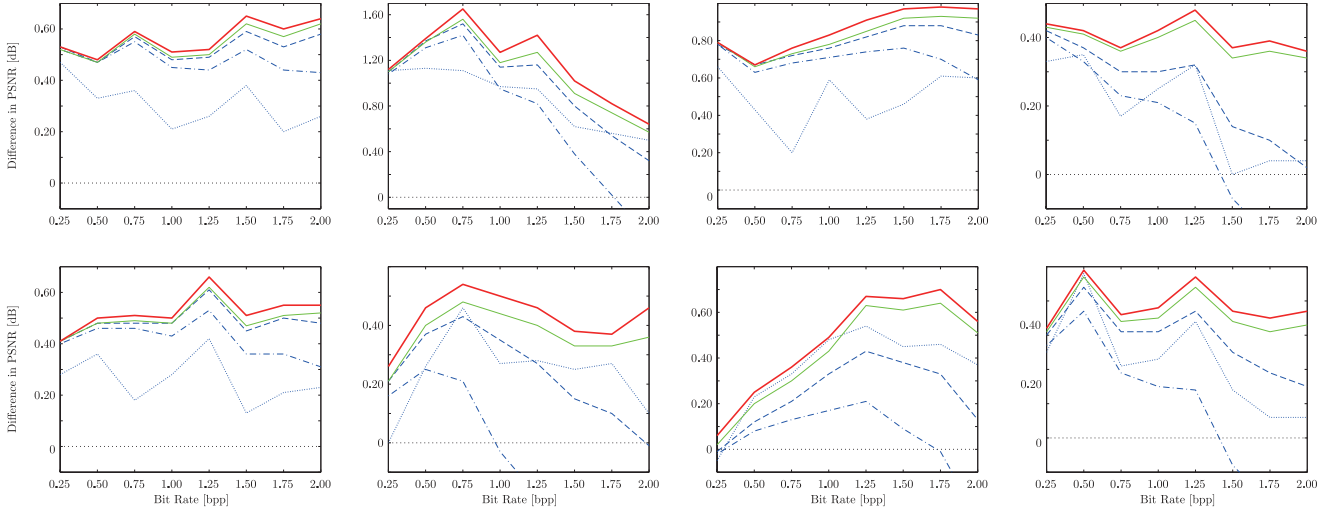


Fig. 4. Results of lossy image coding (blue dotted, blue chained, blue dashed, green solid, and red bold solid lines indicate 8×16 L-LT in [9], 8×16 BL-LT in [11], 8×16 BL-LT in [12], 8×16 DCT-constrained XBL-LT, and 8×16 DCT-unconstrained XBL-LT, respectively): (top) *Baboon*, *Barbara*, *Finger*, and *Goldhill*, (bottom) *Grass*, *Lena*, *Pepper*, and *Tank*.

TABLE III

RESULTS OF LOSSLESS IMAGE CODING (LBR [BPP], (α) AND (β) MEAN DCT-CONSTRAINED AND DCT-UNCONSTRAINED CASES, RESPECTIVELY.)

Test Images	L-LTs		BL-LTs		XBL-LTs	
	[7]	[9]	[11]	[12]	(α)	(β)
<i>Baboon</i>	6.23	6.26	6.21	6.21	6.21	6.20
<i>Barbara</i>	4.96	4.90	4.90	4.86	4.84	4.83
<i>Boat</i>	5.20	5.15	5.16	5.14	5.13	5.12
<i>Elaine</i>	5.27	5.24	5.26	5.23	5.23	5.23
<i>Finger</i>	5.89	5.92	5.84	5.82	5.82	5.82
<i>Finger2</i>	5.62	5.64	5.55	5.53	5.52	5.51
<i>Goldhill</i>	5.12	5.17	5.15	5.12	5.11	5.11
<i>Grass</i>	6.09	6.14	6.08	6.07	6.07	6.06
<i>Lena</i>	4.63	4.64	4.66	4.62	4.61	4.60
<i>Pepper</i>	5.00	4.93	4.96	4.93	4.92	4.91
<i>Room</i>	4.47	4.51	4.55	4.48	4.46	4.44
<i>Sakura</i>	5.94	6.03	5.95	5.93	5.92	5.90
<i>Station</i>	5.16	5.25	5.21	5.16	5.15	5.14
<i>Tank</i>	5.16	5.19	5.18	5.16	5.15	5.15

coder (SPIHT) [16]. The XBL-LTs were compared with the conventional L-LTs by using the lossless bit rate (LBR) and peak-to-noise ratio (PSNR) in lossy-to-lossless image coding:

$$\text{LBR [bpp]} = \frac{\text{Total number of bits [bit]}}{\text{Total number of pixels [pixel]}}$$

$$\text{PSNR [dB]} = 10 \log_{10} \left(\frac{255^2}{\text{MSE}} \right).$$

Table III and Fig. 4 show the results of lossless and lossy image coding. The vertical axes in Fig. 4 are the differences in PSNRs relative to the 4×8 L-LT in [7] for JPEG XR. It is clear that the XBL-LTs outperformed the conventional L-LTs in lossy-to-lossless image coding. In particular, although lifting-based transforms tended to degrade coding performance at high bit rates, the XBL-LTs preserved coding performance even at such high bit rates.

V. CONCLUSION

By extending an original LT and using block-lifting factorization, we developed an XBL-LT with fewer rounding

operations. It is DCT-unconstrained and hence can be DCT-constrained as well; i.e., it can be considered to be a more general structure than other BL-LTs. Although we constrained the design by using unitary matrices in this paper, the DCT-unconstrained structures have the potential to achieve better coding.

ACKNOWLEDGMENT

This work was supported by JSPS Grant-in-Aid for Young Scientists (B), Grant Number 25820152.

REFERENCES

- [1] H. S. Malvar, *Signal Processing with Lapped Transforms*, Norwood, MA: Artech House, 1992.
- [2] K. R. Rao and P. Yip, *Discrete Cosine Transform Algorithms*, Academic Press, 1990.
- [3] G. K. Wallace, "The JPEG still picture compression standard," *IEEE Trans. Consum. Electr.*, vol. 38, no. 1, pp. xviii–xxxiv, Feb. 1992.
- [4] T. Wiegand, G. J. Sullivan, G. Bjøntegaard, and A. Luthra, "Overview of the H.264/AVC video coding standard," *IEEE Trans. Circuits Syst. Video Technol.*, vol. 13, no. 7, pp. 560–576, July 2003.
- [5] G. J. Sullivan, J.-R. Ohm, W.-J. Han, and T. Wiegand, "Overview of the high efficiency video coding (HEVC) standard," *IEEE Trans. Circuits Syst. Video Technol.*, vol. 22, no. 12, pp. 1649–1668, Dec. 2012.
- [6] W. Sweldens, "The lifting scheme: A custom-design construction of biorthogonal wavelets," *Appl. Comput. Harmon. Anal.*, vol. 3, no. 2, pp. 186–200, Apr. 1996.
- [7] C. Tu, S. Srinivasan, G. J. Sullivan, S. Regunathan, and H. S. Malvar, "Low-complexity hierarchical lapped transform for lossy-to-lossless image coding in JPEG XR/HD Photo," in *Proc. of SPIE*, San Diego, CA, Aug. 2008, vol. 7073, pp. 1–12.
- [8] F. Dufaux, G. J. Sullivan, and T. Ebrahimi, "The JPEG XR image coding standard," *IEEE Signal Process. Mag.*, vol. 26, no. 6, pp. 195–199, 204, Nov. 2009.
- [9] T. D. Tran, J. Liang, and C. Tu, "Lapped transform via time-domain pre- and post-filtering," *IEEE Trans. Signal Process.*, vol. 6, no. 6, pp. 1557–1571, June 2003.
- [10] T. Suzuki, M. Ikehara, and T. Q. Nguyen, "Generalized block-lifting factorization of M -channel biorthogonal filter banks for lossy-to-lossless image coding," *IEEE Trans. Image Process.*, vol. 21, no. 7, pp. 3220–3228, July 2012.
- [11] T. Suzuki and M. Ikehara, "Integer fast lapped transforms based on direct-lifting of DCTs for lossy-to-lossless image coding," *EURASIP J. Image. Video Process.*, vol. 2013, no. 65, pp. 1–9, Dec. 2013.

- [12] T. Suzuki and H. Kudo, "Integer fast lapped biorthogonal transform via applications of DCT matrices and dyadic-valued factors for lifting coefficient blocks," in *Proc. of ICIP'13*, Merboulne, Australia, Sep. 2013, pp. 800–804.
- [13] T. Suzuki and M. Ikehara, "Integer DCT based on direct-lifting of DCT-IDCT for lossless-to-lossy image coding," *IEEE Trans. Image Process.*, vol. 19, no. 11, pp. 2958–2965, Nov. 2010.
- [14] G. Strang and T. Nguyen, *Wavelets and Filter Banks*, Wellesley-Cambridge Press, 1996.
- [15] S. Fukuma, K. Ohyama, M. Iwahashi, and N. Kambayashi, "Lossless 8-point fast discrete cosine transform using lossless Hadamard transform," Tech. Rep. of IEICE, DSP99-103, Oct. 1999.
- [16] A. Said and W. A. Pearlman, "A new, fast, and efficient image codec based on set partitioning in hierarchical trees," *IEEE Trans. Circuits Syst. Video Technol.*, vol. 6, no. 3, pp. 243–250, June 1996.